An Experimental Study on Heat Transfer Mechanisms in Microlayer of a Boiling Bubble

Seung Hyuck Chung[a], Satbyoul Jung[a], Hyungdae Kim[a*]
[a]*Department of Nuclear Engineering, Kyung Hee Univ., Republic of Korea*

[*]*Corresponding author: hdkims@khu.ac.kr*

1. Introduction

Nucleate boiling is widely used in practical applications due to its extensive heat transfer. Bubble growth in nucleate boiling is divided into two regions, an inertia-controlled growth region and a diffusion-controlled growth region. Due to rapid bubble growth from high inertial forces and the relatively slow triple contact line movement by viscous stresses at the wall, a thin liquid film appears underneath a boiling bubble on heated wall, which is referred to as microlayer. Evaporation of liquid on the microlayer contributes to the growth of a boiling bubble, resulting in intensive heat transfer from the heated wall. In this regard, a number of theoritical and experimental studies on dynamics and heat transfer characteristics of microlayer have been performed constantly [1-5]. However, there is a lack in interpreting dynamic and thermal behaviors of microlayer with applications to numerical simulation of nucleate boiling. In this study, the heat transfer mechanisms of microlayer proposed in the previous studies are examined using the complete experimental data on dynamic and thermal behavior of microlayer during nucleate boiling – spatially and temporally synchronized surface temperature distribution, liquid-vapor phase distribution, and microlayer geometry during nucleate boiling of a single bubble – which is obtained by the unique experimental technique developed in our laboratory [6, 7].

2. Experiment

2.1 Experimental technique and setup

We consider the experimental setup to simultaneously measure the temperature distribution using infrared thermometry, phase distribution using total reflection, and microlayer geometry using laser interferometry.

An incoherent light source is generally used for conventional total reflection. When a coherent source (i.e., a laser) is used for total reflection, interference patterns appear due to the microlayer beneath the boiling bubble. The fringe spacing between the adjacent light and dark rings is given by

$$\delta_{m+1} - \delta_m = \frac{\lambda}{2n_l \cos\theta_l} \quad (1)$$

where δ_m is the thickness of the microlayer, n_l is the index of refraction of the liquid film layer, θ is the angle of refraction into liquid from the substrate, λ is the wavelength of the laser light, and m is the fringe order.

Transient heat conduction equation for the heater plate was numerically solved by using the measured time-varying temperature distribution data of the boiling surface as boundary conditions using a commercial computational fluid dynamics program and a user defined code which was added to update the temperature boundary condition on the boiling surface for each time step.

To ensure the three optical techniques, a combination of an ITO film heater (transparent to visible light and opaque to infrared light) and a CaF_2 substrate (transparent to both visible and infrared light) was used as a test sample. More detailed experiment technique and setup are given in [6, 7].

2.2 Experimental conditions

The experiment data for nucleate boiling of water was obtained at saturation condition and applied heat flux of 113 kW/m^2 under atmospheric pressure. The spatial and temporal resolutions were 60 μm and 1 ms for the surface temperature and heat flux and 24 μm and 0.1 ms for the phase detection, respectively.

3. Results and Discussions

A set of time- and space-synchronized liquid-vapor phase distribution including microlayer fringe patterns and surface temperature distribution on a heated wall were successfully obtained during single bubble nucleate boiling under atmospheric pressure and saturation condition. The obtained data were systemically analyzed to determine the microlayer geometry and to discuss the associated heat transfer mechanisms underneath a vapor bubble growing on a heated wall during nucleate boiling.

3.1 Geometry and dynamics of microlayer

The history of microlayer geometry can be obtained by analyzing the fringe patterns from the laser interferometry, as seen in Fig. 1. Fig. 2 shows the analysis results of microlayer geometry. It is found that the maximum microlayer thickness for water at average heat flux of 113 kW/m^2 is approximately 3.5 μm while it is spread over the extended region with a width of

several hundred μm, and that the angle of the microlayer wedge is very small at about 0.3°. In the extended liquid microlayer where effects of disjoining pressure, vapor recoil pressure, and interfacial resistance are negligible, heat is transferred from a heated wall through the microlayer to a vapor bubble [8]. This region is of interest in the present study.

In addition to the present study, there have been several experimental measurements of microlayer geometry using laser interferometry [1-4]. A comparison of these results and the data in previous experimental studies is given in Fig. 2, where the measured thickness at the outer edge of the microlayer as a function of dimensionless time normalized to the microlayer depletion time, t_d, is plotted. Although the experiments were conducted with different fluids and under different conditions, there is good agreement in order of magnitude and trends.

3.2 Evaporation heat flux on the microlayer

When a microlayer expands beneath a boiling bubble, superheated liquid in the microlayer evaporates quickly, contributing to bubble growth and heat transfer from the wall [1, 3]. The local heat flux due to microlayer evaporation can be calculated with Eq. (2) and the history of microlayer geometry.

$$q''_{evap}(r,t) = \rho_f h_{fg} \frac{\partial \delta(r,t)}{\partial t} \tag{2}$$

where ρ_f is the liquid density, h_{fg} is the heat of vaporization, δ is the thickness of the liquid layer. The space-averaged heat flux of microlayer evaporation as a function of non-dimensional time is plotted in Fig. 4. In the same manner, the experimental data from the previous studies was also added to the plot for comparison. The results in the present study show the decrease tendency from 1000 kW/m^2 to 200 kW/m^2 with time. It is interesting that the space-averaged heat flux data shows fairly good agreement, within an order of magnitude, although there are differences in working fluids and experimental conditions.

3.3 Wall heat flux underneath microlayer

In this section we consider heat transfer from a heated wall to the microlayer underneath a boiling bubble. The surface temperature and local heat flux distributions obtained from the infrared thermometry and transient conduction analysis enable discussion of how thermal energy is transferred from the heated wall to the growing bubble. The heat flux from the heated wall to the microlayer is calculated using the temperature gradient at the boiling surface (z = 0) as:

$$q''_{wall} = -k \frac{\partial T(x,y,z,t)}{\partial z}\bigg|_{z=0} \tag{3}$$

where k is the thermal conductivity of the solid and T(x, y, z, t) is the three-dimensional temperature distribution of the heated wall, which is the solution of the transient heat conduction analysis. It is found that while it is hard to determine the microlayer region using the temperature distribution result, there is a strong correspondence between the microlayer area and the high heat flux region.

Fig. 4 shows evolution of the local wall heat flux as a function of dimensionless time normalized to bubble departure time, t_D, at a point near the center (r = 0.3 mm) under a boiling bubble. Similar wall heat flux data obtained from previous studies is included in the plot to validate the general trend of the present data. Cooper [5] deduced the wall heat flux by applying one-dimensional heat conduction analysis to the wall temperature-time history, which was measured using micro-sized thermometers mounted at the boiling surface.

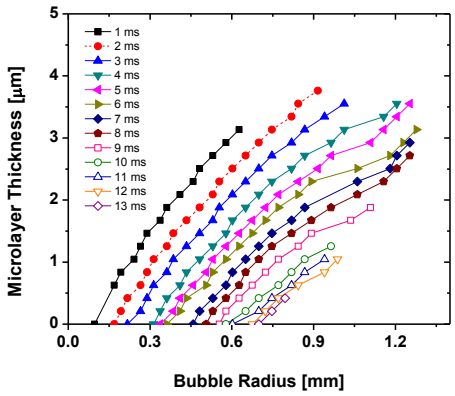

Fig. 1. Time evolution of microlayer geometry beneath a growing bubble

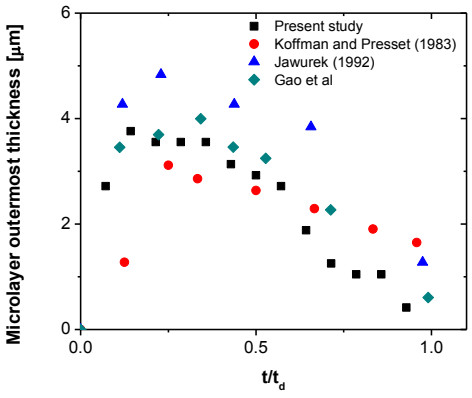

Fig. 2. Time evolution of the maximum microlayer thickness

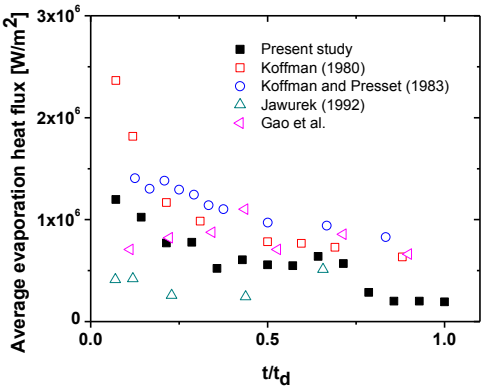

Fig. 3. Time evolution of space-average heat flux of microlayer evaporation

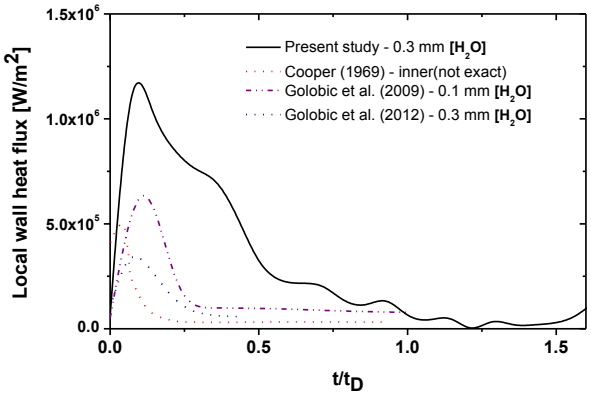

Fig. 4. Local wall heat flux history at a position near the cavity of a nucleating bubble. The number in the legend indicates the distance from the bubble center at which the wall heat flux is measured

The results showed about ten times higher heat flux compared to the average heat flux (~1000 kW/m^2 vs. ~100 kW/m^2). On the ground of appearance of such a high heat flux underneath a growing bubble, the author argued that a highly evaporative thin liquid film exists beneath a boiling bubble. Golobic et al. [9, 10] measured the temperature distribution at the under surface of a thin-foil metal heater using a high speed infrared camera and calculated the local heat flux using the lumped capacitance method by assuming that lateral heat conduction in the thin-foil metal heater is negligible relative to the heat transfer to the bubble. The measure was conducted for saturated water under atmospheric pressure at an average input heat flux of 50, 100 kW/m^2, similar to present experimental conditions. The wall heat flux history at a local point underneath a growing bubble shows fairly good agreement in magnitude and trends, as shown in Fig. 4.

3.4 Conduction heat transfer across microlayer

Cooper [5] and Guion et al. [8] analytically showed that the heat capacity of the microlayer and interfacial resistance are negligible ($k_l \frac{d^2T}{dz^2} >> \rho c_p \frac{dT}{dt}$; $T_i = T_{sat}$) and that no liquid flow can be assumed in the microlayer. Therefore, the conduction heat flux through the microlayer can be expressed in the form of a one-dimensional steady-state conduction equation as:

$$q''_{cond} = \frac{k_l}{\delta}(T_w - T_{sat}) \tag{4}$$

where k_l is the thermal conductivity of the liquid.

Since the surface temperature and the microlayer thickness are measured, the conduction heat flux across the microlayer can be calculated using Eq. (4). Figure 5 shows the conduction heat flux distribution in the microlayer as well as those for microlayer evaporation and conduction in the solid wall for three time steps of 2 ms, 4 ms, and 6 ms. It is found that the microlayer evaporation and wall conduction heat flux profiles are in good agreement. In addition, the microlayer conduction result has a consistency in an order of magnitude from the others.

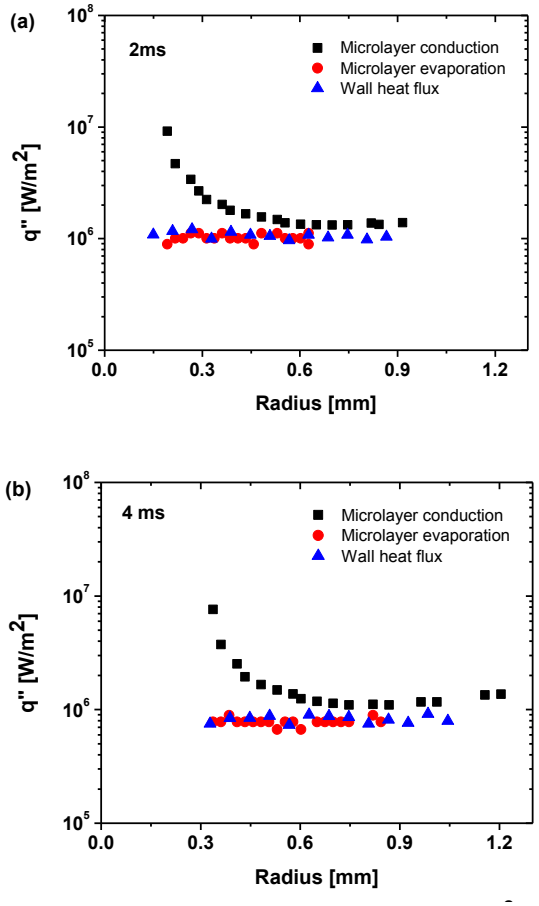

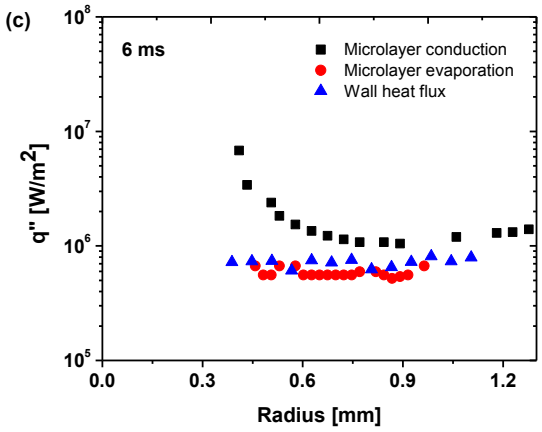

Fig. 5. Plot of heat flux profiles for microlayer evaporation, transient wall conduction, conduction across the microlayer: (a) 1 ms, (b) 2 ms, (c) 3 ms

4. Conclusions

The detailed geometry of microlayer and the associated heat transfer mechanisms underneath a boiling bubble under atmospheric pressure and saturation condition at an average heat flux of 133 kW/m^2 were investigated with results from an experimental method to spatially and temporally synchronize the surface temperature distribution, the liquid-vapor phase distribution, and the microlayer geometry. The findings from this study are as follows:

- The thickness of the extended liquid microlayer observed underneath a vapor bubble is order of a few of μm while the width is order of hundreds of μm. The angle of the microalyer wedge is less than 0.3°.
- The evaporation heat flux was calculated by knowing microlayer thickness. The space-averaged values decreased from 1200 to 200 kW/m^2 with time.
- The wall heat flux was calculated by numerically solving the three-dimensional transient heat conduction using the temperature distribution in each time step. The obtained values were almost 1000 kW/m^2.
- The conduction heat flux was calculated by solving the steady-state one-dimensional heat conduction with the surface temperature and microlayer thickness.
- The three major heat transfer mechanisms associated with the extended microlayer, including the heat flux of microlayer evaporation, the wall heat flux beneath the microlayer, and the conduction heat flux across the microlayer, show a fairly good agreement in order of magnitude.

REFERENCES

[1] L. D. Koffman, M. S. Plesset, Experimental observations of the microlayer in vapor bubble growth on a heated solid, Journal of Heat Transfer, Vol. 105, p. 625-632, 1983
[2] L. D. Koffman, Experimental observations of the microlayer in vapor bubble growth on a heated sold, Ph. D. Thesis, California Institute of Technology, Pasadena, California, 1980
[3] H.H Jawurek, Simultaneous determination of microlayer geometry and bubble growth in nucleate boiling, Int. J. Heat Mass Transfer, Vol. 12, p. 843-846, 1969
[4] M. Gao, L. Zhang, P. Cheng, X. Quan, An investigation of microlayer beneath nucleation bubble by laser interferometric method, Int. J. Heat and Mass Transfer, Vol. 57, p. 183-189, 2012
[5] M. G. Cooper and A. J. P. Lloyd, The microlayer in nucleate pool boiling, Int. J Heat Mass Transfer, Vol. 12, p. 895-913, 1969
[6] Jung. S., Kim. H., An experimental method to simultaneously measure the dynamics and heat transfer associated with a single bubble during nucleate boiling on a horizontal surface, Int. J. Heat and Mass Transfer, Vol. 73, p. 365-375, 2014
[7] Jung. S, Kim. H, Simultaneous investigation of dynamics and heat transfer associated with a single bubble nucleate boiling, Transactions of the Korean Nuclear Society Autumn Meeting, 2013
[8] A. Guion, D. Langewisch, J. Buongiorno, Proc. of 8th Int. Conference on Multiphase Flow, ICMF2013-528, p. 1-10, 2013
[9] I. Golobic, J. Petkovsek, M. Baselj, A. Papez, D. B. R. Kenning, Experimental determination of transient wall temperature distribution close to growing vapor bubbles, Heat and Mass Transfer, Vol. 45, p. 857-866, 2009
[10] I. Golobic, J. Petkovsek, M. Baselj, A. Papez, D. B. R. Kenning, Bubble growth and horizontal coalescence in saturated pool boiling on a titanium foil, investigated by high-speed IR thermography, Int. J. Heat and Mass Transfer, Vol. 55, p. 1385-1402, 2012